TELKOMNIKA, Vol. 13, No. 4, December 2015, pp. 1204~1213
ISSN: 1693-6930, accredited A by DIKTI, Decree No: 58/DIKTI/Kep/2013
DOI: 10.12928/TELKOMNIKA.v13i4.3165

Current Ripple Analysis of New Double-Stator AC Drive Systems

Irham Fadlika[1], AN Afandi[2], Pekik Argo Dahono[3]
[12]Universitas Negeri Malang, Jalan Semarang 5 Malang, Indonesia
[3]Institut Teknologi Bandung, Jalan Ganesha 10 Bandung, Indonesia
e-mail: irham.elektro.um@gmail.com[1], an.afandi@ieee.org[2], pekik@konversi.ee.itb.ac.id[3]

Abstract

This paper presents a current ripple analysis of new double-stator AC drive system. At first, a new double-stator AC drive system is proposed. The aim is to combine the benefits both the multilevel and multiphase system to provide the better performance to drive AC motor. The input and output current ripples of the proposed AC drive system are then analyzed. The current ripples of the proposed AC drive system are then compared to the ones of conventional double-stator AC drive system. Under the same DC input voltage, it is shown that the proposed results in less output current ripple. Under the same output voltage, the proposed AC drive system results in smaller input current and, therefore, fewer losses on the DC power supply. Experimental results are included to show the validity of the proposed concept.

Keywords*: Inverter, AC drive, multiphase*

1. Introduction

Many studies have been conducted to improve the performance of AC drive system. With advanced progress of the power semiconductor switches, inverters can widely applied as AC drive with high-frequency switching and various levels of power requirements [1]-[4]. Various kinds of AC drive system topology by using an inverter has been researched and developed for a wide variety of applications, such as locomotive traction, electric ship propulsion, more-electric aircraft, and high-power industrial applications. For higher power requirements, multiphase and multilevel inverter is the most commonly used. The multiphase inverter basically consists of conventional *n*-half bridge inverter connected in parallel corresponding to the load supplies. It provides lower pulsating torque, better tolerance and the possibility of splitting motor current across a higher number of phases, thus reducing the converter rating [3], [5]-[7]. For high voltage applications, multilevel inverter is more suitable because the inverter output voltage is obtained through a few steps of voltage levels, although it also has some drawbacks. Multilevel system requires a lot of switches and has capacitor voltage unbalanced problem [8]-[11].

In order to develop better performance of the AC drive system as Figure 1, some investigations have been done for both multiphase and multilevel system. Those are focusing to the input [12]-[17], [18], [20] and output [18]-[21] ripple to meet the standard that have been determined [22]. On the input side of the inverter, the current ripple determines the size of the DC link capacitor of the inverter. It has been reported that the DC link capacitor is the most vulnerable component in an inverter. Furthermore, on the output side of the inverter, the higher current ripple could cause the motor to heat faster.

In this paper, a new topology of double-stator AC drive system is proposed to combine the benefits of both multiphase and multilevel system. In the proposed system, as shown in Figure 2, two conventional two-level three-phase inverters are connected in series on the DC sides. Each three-phase output of these two inverters is supplying three-phase stator winding set of double-stator AC motor. By using the proposed topology, the advantages of simple two-level inverter topology and high reliability and power density of multiphase AC motors can be combined. Analytical expressions of input and output current ripples of the proposed system are then derived. It is shown that under the same DC input voltages, the output current ripple of the proposed system is lower than the conventional topology. Under the same output voltage, the proposed system has lower input current and therefore, fewer losses on the DC power supply

Received August 23, 2015; Revised November 12, 2015; Accepted November 29, 2015

than the conventional ones. Experimental results are included to show the validity of the proposed concept. The proposed concept can be extended to higher phase number.

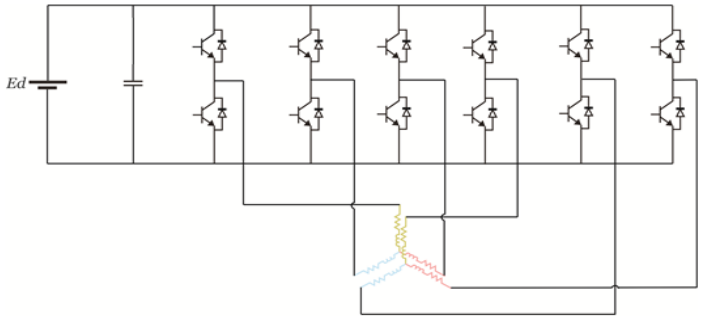

Figure 1. Conventional double-stator AC drive system

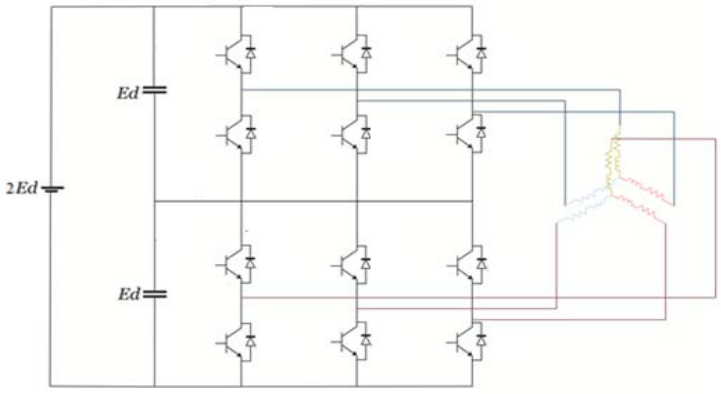

Figure 2. New double-stator AC drive system

2. Proposed Method

In a conventional double stator AC drive system, an AC motor that having two three-phase stator winding sets is used. The neutrals of two winding sets are separated. The two stator winding sets are supplied by two two-level three-phase inverters as shown in Figure 1. The two three-phase inverters are supplied by a common DC voltage source. These two stator winding sets can be displaced by various angles. In this paper, only zero angle displacement is discussed. The main problems of this conventional system is the increasing DC input current with the associated large DC supply losses.

In order to solve the mentioned problem, a new topology as shown in Figure 2 is proposed. In the proposed system, the two three-phase inverters are connected in series. As the input voltage is connected in series, the required DC input current is lower than the conventional ones. PWM techniques for the new topology and the conventional ones are the same.

3. Input Current Ripple of New Double-Stator AC Drive System

Input current ripple analysis is very important in designing the required DC filter capacitor. In the new topology, the input current of the upper side inverter can be expressed as,

$$i_d = i_{u_1}.s_{u_1} + i_{v_1}.s_{v_1} + i_{w_1}.s_{w_1} \quad (1)$$

where s_{u1}, s_{v1}, and $s_{w1}$is switching states of phases u_1, v_1, and w_1, respectively. The value of switching state is unity (zero) when the upper switching device of the associated phase receives an ON (OFF) signal. The output currents are assumed to be balanced and sinusoidal:

$$\begin{aligned} i_{u_1} &= \sqrt{2} I_l \sin(\theta_r - \phi) \\ i_{v_1} &= \sqrt{2} I_l \sin(\theta_r - \frac{2\pi}{3} - \phi) \\ i_{w_1} &= \sqrt{2} I_l \sin(\theta_r + \frac{2\pi}{3} - \phi), \end{aligned} \quad (2)$$

where φ is the load phase angle, $\theta_r = 2\pi f_r t = \omega t$, f_r is the fundamental output frequency of the inverter and I_l is the rms value of the load current.

In carrier based PWM inverter, the ON and OFF signals for the inverter switching devices are obtained by comparing a three-phase reference signal to a high-frequency triangular carrier signal with unity amplitude. The upper inverter switching device receives an ON (OFF) signal whenever the associated reference signal is higher (lower) than the triangular signal. If the frequency of the carrier signal is much higher than the reference one, the values of the reference signals in one carrier period can be assumed as constants. By using this assumption, the detailed inverter waveforms over one carrier period can be drawn as shown in Figure. 3.

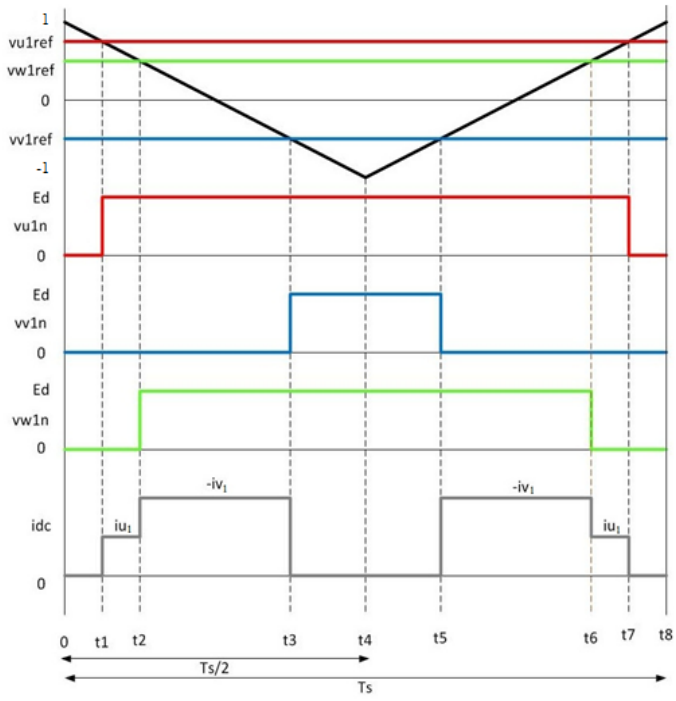

Figure 3. Inverter waveforms in one carrier period

The time intervals in Figure 3 can be obtained as follows:

$$\begin{aligned} \frac{t_1}{T_s/2} &= \frac{1 - {v_u}^r}{2} \\ \frac{t_2}{T_s/2} &= \frac{1 - {v_w}^r}{2} \\ \frac{t_3}{T_s/2} &= \frac{1 - {v_v}^r}{2} \end{aligned} \quad (3)$$

where,

$$\begin{aligned} v_u^r &= k \sin\ \theta_r \\ v_v^r &= k\ \sin\left(\theta_r - \tfrac{2\pi}{3}\right) \\ v_w^r &= k\ \sin\left(\theta_r + \frac{2\pi}{3}\right) \end{aligned} \quad (4)$$

Based on Figure. 3, the inverter input current in one carrier period can be written as follow:

$$i_d = \begin{cases} 0 & 0 \le t \le t_1 \\ i_{u_1} & t_1 \le t \le t_2 \\ -i_{v_1} & t_2 \le t \le t_3 \\ 0 & t_3 \le t \le t_4 \\ -i_{v_1} & t_4 \le t \le t_5 \\ i_{u_1} & t_5 \le t \le t_6 \\ 0 & t_6 \le t \le t_7 \end{cases} \quad (5)$$

The mean square value of the inverter input current over one carrier period can be obtained as follow:

$$\begin{aligned} {I^2}_{d_1} &= \tfrac{1}{T_s}\int_{t_0}^{t_0+T_s} {i_d}^2 dt \\ &= \frac{2(t_1 - t_2)}{T_s}{i_{u_1}}^2 + \frac{2(t_3 - t_2)}{T_s}{i_{v_1}}^2 \end{aligned} \quad (6)$$

Substituting (2) and (3) into (5) and the result is substituted into (6) then the following is obtained

$$\begin{aligned} {I^2}_{d_1} &= 2{I_l}^2 \sin^2(\omega t - \phi)\tfrac{\sqrt{3}}{2} k \sin\left(\omega t - \tfrac{\pi}{6}\right) \\ &+ 2{I_l}^2 \sin^2(\omega t - \frac{2\pi}{3} - \phi)\frac{\sqrt{3}}{2} k \sin\left(\omega t + \frac{\pi}{2}\right) \end{aligned} \quad (7)$$

The average value of the mean square of the inverter input current over one fundamental inverter period can be obtained as follow:

$$\begin{aligned} {I^2}_{d_1,av} &= \tfrac{3}{\pi}\int_{\frac{\pi}{6}}^{\frac{\pi}{2}} I_d^2\, d(\omega t) \\ {I^2}_{d_1,av} &= \frac{3\sqrt{3}}{2\pi} k I_l^2 \left[1 + \frac{2}{3}\cos 2\phi\right] \end{aligned} \quad (8)$$

As the inverter operation is symmetrical, the integral operation can be performed just over 60^o period.

If the inverter losses can be neglected, the DC component of the inverter input current can be obtained by equalizing the inverter input and output powers and, the result is

$$\overline{i_d} = \tfrac{3}{\sqrt{2}}.k.I_l.\cos\phi \quad (9)$$

Based on (8) and (9) then the ripple component of the inverter input current can be determined as follow:

$$\widetilde{i_{d_1}} = \sqrt{{I^2}_{d_1,av} - {\overline{I_d}}^2} \quad (10)$$

$$\widetilde{i_{d_1}} = I_l \sqrt{k\left[\frac{\sqrt{3}}{2\pi} + \left(\frac{\sqrt{3}}{2\pi} - \frac{9}{8}k\right)\cos^2\phi\right]}$$

4. Output Current Ripple of New Double-Stator AC Drive System

For output current ripple analysis, it is assumed that the load can be represented as shown in Figure 4.

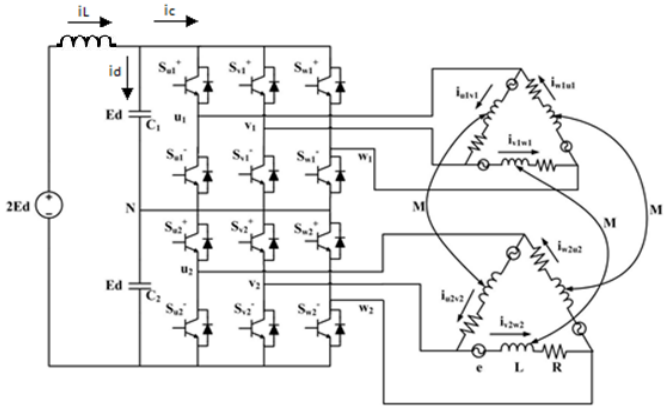

Figure 4. New double-stator AC drive system with delta load

Based on the circuit in Figure 4, the voltage differences between phases $u_1$and v_1 and between u_2 and v_2 can be expressed as follow

$$v_{u_1v_1} = Ri_{u_1v_1} + L\frac{d}{dt}i_{u_1v_1} + M\frac{d}{dt}i_{u_2v_2} + e_{u_1v_1} \quad (11)$$

$$v_{u_2v_2} = Ri_{u_2v_2} + L\frac{d}{dt}i_{u_2v_2} + M\frac{d}{dt}i_{u_1v_1} + e_{u_2v_2}$$

The inverter output voltage and current can be decomposed into the average (average over one carrier period) and ripple components. By neglecting the ripple voltage drop across the load resistances then the ripple component of the load currents can be expressed as follows:

$$\tilde{\imath}_{u_1v_1} = \frac{1}{L+M}\int\left(v_{u_1v_1} - \tilde{v}_{u_1v_1}\right)dt \quad (12)$$

where tilde denoting ripple component.

Based on the inverter voltage waveforms as shown in Figure 5, then the detailed output current ripple over one carrier period can be written as

$$\tilde{\imath}_{u_1v_1} = \frac{1}{L+M}\begin{cases} \bar{v}_{un}(-t) - (\bar{v}_{vn}(-t)) & 0 \le t \le t_1 \\ \bar{v}_{un}(-t) - (\bar{v}_{vn}(-t)) & t_1 \le t \le t_2 \\ (\bar{v}_{un}(\left(\frac{E_d}{\bar{v}_{un}} - 1\right)(t-t_2) - t_2) - (\bar{v}_{vn}(-t)) & t_2 \le t \le t_3 \\ (\bar{v}_{un}(\left(\frac{E_d}{\bar{v}_{un}} - 1\right)(t-t_2) - t_2) - (\bar{v}_{vn}(\left(\frac{E_d}{\bar{v}_{vn}} - 1\right)(t-t_3) - t_3) & t_3 \le t \le \frac{T_s}{2} \end{cases}$$

(13)

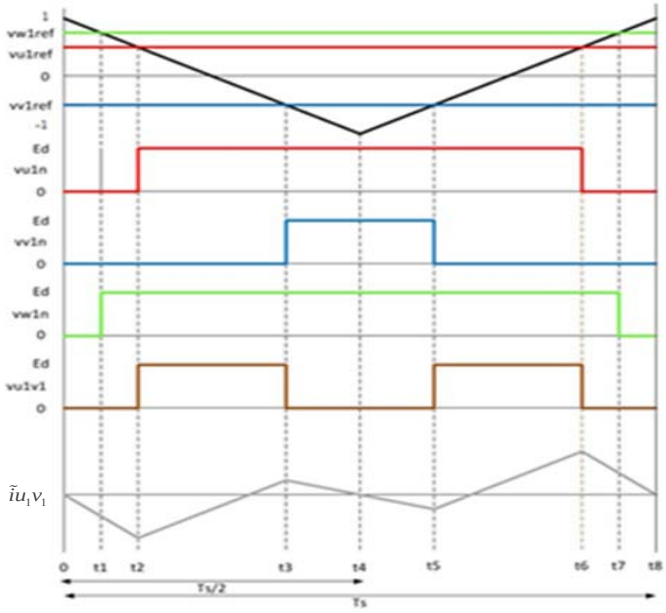

Figure 5. Inverter waveforms in one carrier period

where

$$\bar{v}_{u_1n} = \frac{T_s/2 - t_2}{T_s/4} E_d$$
$$\bar{v}_{v_1n} = \frac{T_s/2 - t_3}{T_s/4} (E_d) \quad (14)$$
$$\bar{v}_{wn} = \frac{T_s/2 - t_1}{T_s/4} (-E_d)$$

The mean square value of the output current ripple over one carrier period can be determined as follow:

$$\tilde{I}_{uv}{}^2 = \frac{1}{T_s}\int_0^{T_s} \tilde{i_{uv}}{}^2 dt = \frac{2}{T_s}\int_0^{T_s/2} \tilde{i}_{uv}{}^2 dt \quad (15)$$

Substituting (13) and (14) into (15) then and performing the integration the results as shown in Table 1 are obtained.

Table 1.Output current ripple for one switching period

Area A1 (0≤ωt≤π/6)	$\frac{\mathbf{Ed^2 k^2 Ts^2 (Cos[\frac{1}{6}(\pi - 6\theta)] + Sin\theta)^2 (4 + 3k^2 - 2\sqrt{3}kCos\theta - 6kSin\theta)}}{\mathbf{768(L+M)^2}}$
Area A2 (π/6≤ωt≤π/2)	$\frac{\mathbf{Ed^2 k^2 Ts^2 (Cos[\frac{1}{6}(\pi - 6\theta)] + Sin\theta)^2 (4 + 3k^2 - 2\sqrt{3}kCos\theta - 6kSin\theta)}}{\mathbf{768(L+M)^2}}$

The average value of the mean square of the inverter output current over one fundamental inverter period can be obtained as follow:

$$\tilde{I}_{uv,rms}{}^2 = \frac{1}{\pi/2}\int_0^{\pi/2} \tilde{I}_{uv}{}^2 d\theta \quad (16)$$

As the inverter operation is symmetrical, the integral operation can be performed just over 90^o period. Then the ripple component of the inverter output current can be determined as follow:

$$\tilde{I}_{u_1v_1,rms}{}^2 = \frac{(\mathrm{Ed}^2k^2(12(\sqrt{3}+\pi)+k(-54-22\sqrt{3}+9k(\sqrt{3}+\pi)))\mathrm{Ts}^2)}{1536(L+M)^2\pi} \quad (17)$$

where
E_d = DC voltage source of inverter
T_s = Switching period
L = Load inductance
M = Mutual leakage inductance
k = Modulation index

5. Results and Discussion

A small experimental system was constructed to verify the proposed concept. The DC voltage source is obtained by rectifying three-phase AC voltage source. The inverter switching devices are implemented by using power MOSFET. The load resistance and inductance are 1.26 Ohm and 5.62 mH, respectively. The mutual leakage inductance can be neglected. The DC voltage source E_d is maintained constant at 26.25 Vdc. The switching devices are switched at 1000 Hz. The fundamental output frequency is 50 Hz.

The validity of the analysis of the input and output current ripple of the proposed system is shown in Figure 6 and 7. From Figure 8-11, input and output current ripple comparison between proposed and conventional multiphase system are shown. Under the same input voltage, shown in Figure 8-9, input current ripple of both system are the same, but the output current ripple of the proposed system is lower. Under the same output voltage, shown in Figure 9-11, output current ripple of both system are the same, but the input current ripple of the proposed system is lower. Accuracy of the proposed analysis method can be appreciated from these figures.

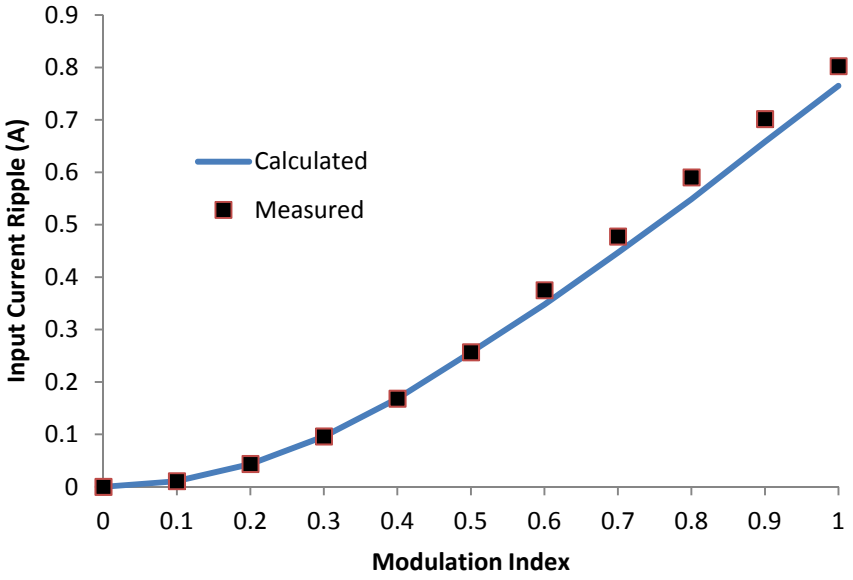

Figure 6. Input current ripple of the proposed topology

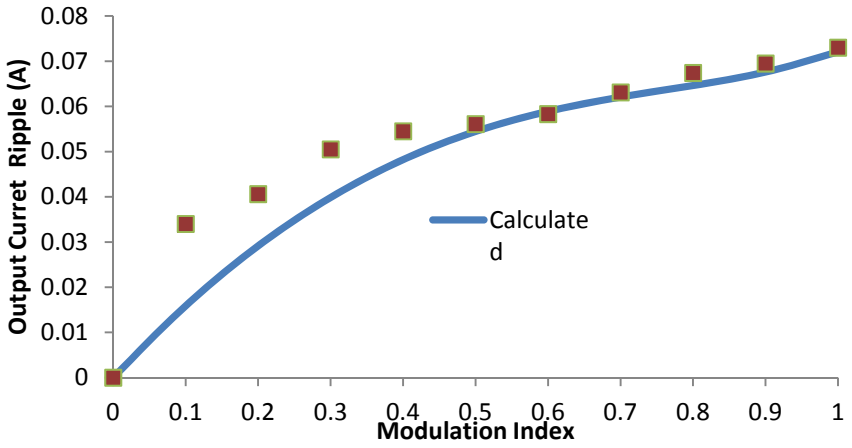

Figure 7. Output current ripple of the proposed topology

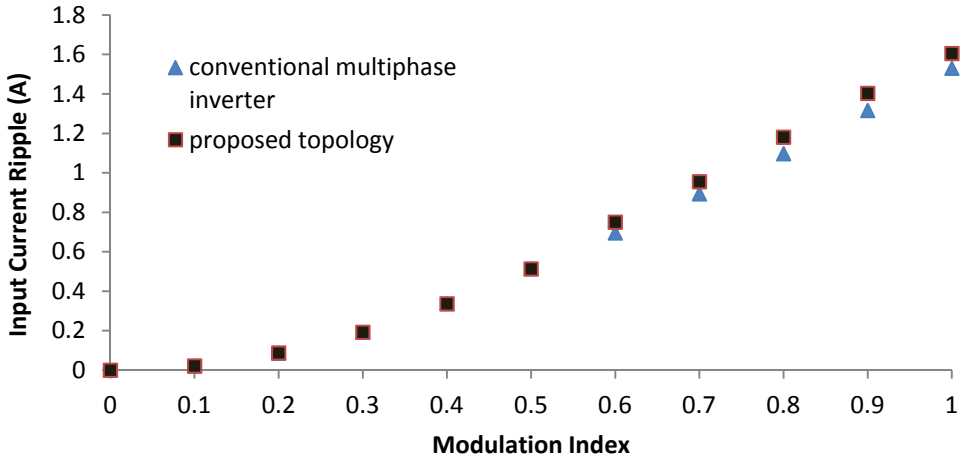

Figure 8. Input current ripple comparison between conventional multiphase inverter and proposed topology under the same DC input voltage

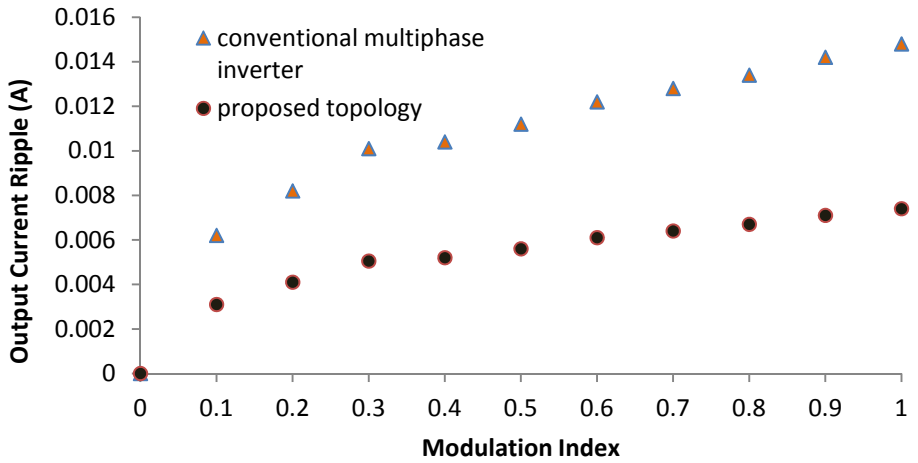

Figure 9. Output current ripple comparison between conventional multiphase inverter and proposed topology under the same DC input voltage

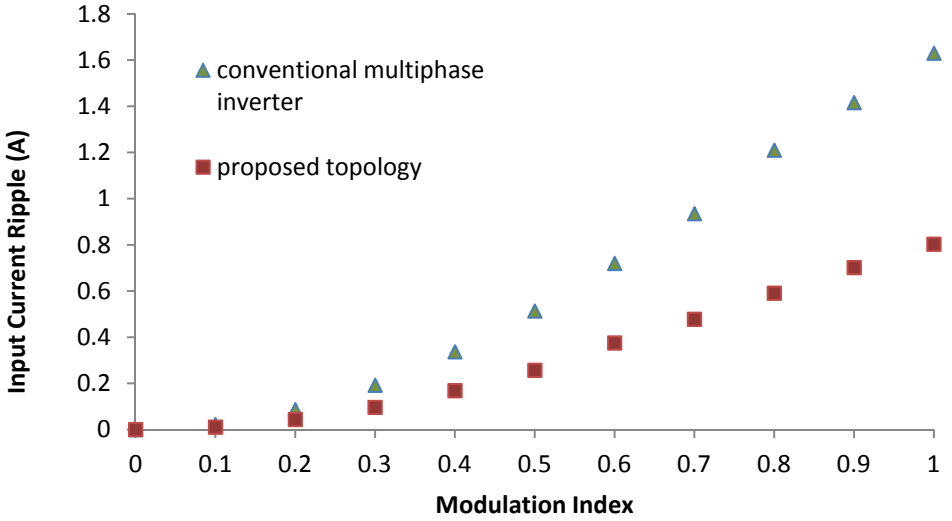

Figure 10. Input current ripple comparison between conventional multiphase inverter and proposed topology under the same output voltage

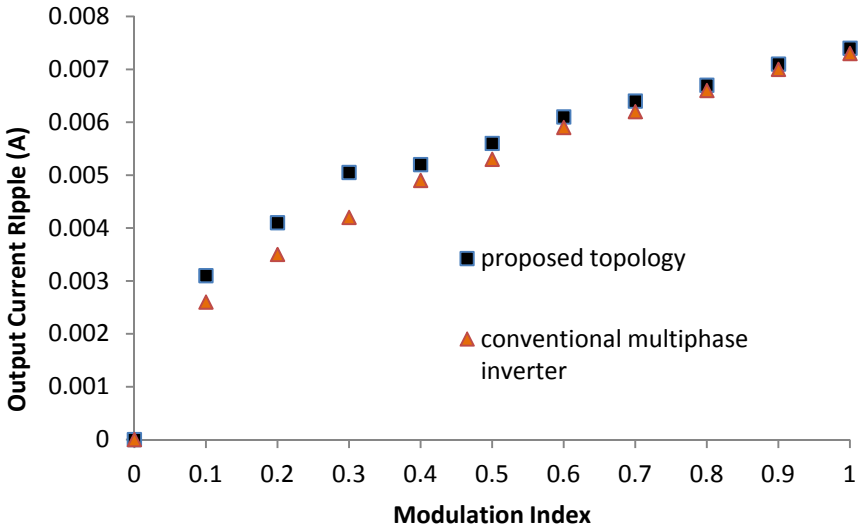

Figure 11. Output current ripple comparison between conventional multiphase inverter and proposed topology under the same output voltage

6. Conclusion

In this paper, analytical expressions for total input and output current ripple of a new double-stator AC drive system have been derived and proved by experiment. The derived expressions are useful in designing DC input and output filters. It is expected that the proposed topology can be used as an alternative to the conventional topology.

References

[1] Chengsheng W, Chongjian L, Li L, Chunyi Z, Zhiming Z. Investigation on large power AC drive system. IEEE 8th *International Conference on Power Electronics and ECCE Asia (ICPE & ECCE)*. 2011.

[2] Levi E. *Recent Developments in High Performance Variable-Speed Multiphase Induction Motor Drives.* 6th Int'l. Symposium Nikola Tesla. 2006.

[3] Levi E. Multiphase Electric Machines for Variable-Speed Applications. *IEEE Trans. Ind. Electr*. 2008; 55(5).
[4] Wu B. *High Power Converter and AC Drives*. IEEE Press, Piscataway, NJ. 2006.
[5] Williamson S, Smith S. Pulsating Torque and Losses in Multiphase Induction Machines. *IEEE Trans. Ind. Appl*. 2013; 39(4).
[6] Klingshirn EA. High Phase Order Induction Motors Part I: Description and Theoretical Consideration. *IEEE Trans. Power App. Syst*. 1983; PAS-102: 47-53.
[7] Nelson RH, Krause PC. *I*nduction Machine Analysis for Arbitrary Displacement Between Multiple Winding Sets. *IEEE Tran. Power App. Sys*. 1974; PAS-93(3).
[8] Peng FZ, Wei Q, Dong C. Recent Advances in Multilevel Converter/Inverter Topologies and Applications. *International Power Electronics Conference (IPEC)*. 2010.
[9] Omar R, Rasheed M, Sulaiman M. Comparative Study of a Three Phase Cascaded H-Bridge Multilevel Inverter for Harmonic Reduction. *TELKOMNIKA Indonesian Journal of Electrical Engineering*. 2015; 14(3): 481 ~ 492.
[10] Kiruthika P, Kannan R. Multi-Carrier based 27-level Hybrid Multi-level Inverter Interface with PhotoVoltaic. *TELKOMNIKA Indonesian Journal of Electrical Engineering*. 2015; 13(3): 467 ~ 475.
[11] Pan W, Fei L, Xiaoming Z, Jianhua Y, Xiangbing W. Research on a New Type of Energy Feedback Cascade Multilevel Inverter System. *TELKOMNIKA*. 2013; 11(1): 494~502.
[12] Ziogas P, Photiadis PND. An Exact Input Current Analysis of Ideal Static PWM Inverters. *IEEE. Trans. on Industrial Applications.* 1983; 1A -19(2).
[13] Dahono PA, Sato Y, Kataoka T. *Analysis and Minimization of Ripple Components of Input Current and Voltage of PWM Inverters*. Industry Applications Conference, 1995. Thirtieth IAS Annual Meeting, IAS '95, Conference Record of the 1995 IEEE.
[14] Parlindungan RS, Dahono PA. Input Current Ripple Analysis of Double Stator AC Drive Systems. *International Conference on Information Technology and Electrical Engineering (ICITEE)*. 2013.
[15] Dahono PA, Satria A. Input Current Ripple Analysis of Inverter Fed Dual Three-Phase AC Motors. *Power Electronics Conference* (IPEC-Hiroshima 2014 - ECCE-ASIA), 2014.
[16] Nurafiat D, Dahono PA. Input Current-Ripple Analysis of Nine-Phase PWM Inverter. *International Conference on Electrical Engineering and Informatics (ICEEI).* 2011.
[17] Dahono PA, Deni, Rizqiawan A. Analysis and Minimization of Input Current and Voltage Ripples of Five-Phase PWM Inverters. *IEEE 2nd International Power and Energy Conference*, 2008. PECon 2008.
[18] Dahono PA, Sato Y, Kataoka T. Analysis and Minimization of Harmonics in the AC and DC Sides of PWM Inverters. *IEE Japan Trans. Ind. Appl*. 1995.
[19] Dahono PA. Analysis and Minimization of Output Current Ripple of Multiphase PWM Inverters. *Power Electronics Specialists Conference*, 2006. PESC '06. 37th IEEE
[20] Dahono PA, Sato Y, Kataoka T. *A Novel Method for Analysis of Inverter Currents*. Power Electronics and Variable-Speed Drives, 1994. Fifth International Conference. 1994.
[21] Deni, Supriatna EG, Dahono PA. Output Current Ripple Analysis of Five-Phase PWM Inverters. 7th *International Conference on Power Electronics and Drive Systems*, 2007. PEDS '07.
[22] Lockley B, Wood B, Paes R, Dewinter F. *IEEE Std 1566 - The Need for a Large Adjustable Speed Drive Standard*, Petroleum and Chemical Industry Conference, 2006. PCIC '06. Record of Conference Papers - IEEE Industry Applications Society 53rd Annual.